Impact of the November/December Arctic Oscillation on the following January temperature in East Asia

Shengping He[1,2,3] and Huijun Wang[1,2]

Received 8 July 2013; revised 18 November 2013; accepted 19 November 2013; published 9 December 2013.

[1] We investigated the impacts of the preceding Arctic Oscillation (AO) on winter East Asian temperature (T_{EA}) and the possible mechanisms. It was found that the correlation of the November AO (Nov AO) with the following January T_{EA} is more significant than that with the following December and February T_{EA}. Moreover, the January T_{EA} is also closely related to the preceding December AO (Dec AO). Further analysis revealed that a Rossby wave associated with the Nov AO is confined to high latitudes in December but shifts southeastward to East Asia in January. Similarly, the Dec AO-related wave activities propagating southeastward to East Asia could persist into the following January. Consequently, the signals of the Nov/Dec AO could be transmitted to the following January. Besides, an air-sea interaction might exist over the North Pacific (NP). The sea surface temperature (SST) over the central subtropical NP (west coast of North America) often rapidly rises (drops) a month later and peaks in the following January when the preceding Nov/Dec AO is in positive phase, causing horseshoe SST anomalies (SSTAs) to form in the NP, with positive SSTAs located in the central subtropical NP and surrounded by negative ones. Such a horseshoe SSTA could lead to a strengthening of the air temperature gradient in the north and a weakening in the south due to effective turbulent mixing in the boundary layer. A huge anomalous anticyclone therefore emerges in the NP and favors a weaker East Asian winter monsoon. Warmer January T_{EA} is eventually generated.

Citation: He, S., and H. Wang (2013), Impact of the November/December Arctic Oscillation on the following January temperature in East Asia, *J. Geophys. Res. Atmos.*, *118*, 12,981–12,998, doi:10.1002/2013JD020525.

1. Introduction

[2] Owing to a lack of maritime influence from the westerly winds that prevail in Europe, it is much colder on the East Asian continent than other regions at similar latitudes, except for northeastern North America in boreal winter. As cold surges are the most profound climate feature in boreal winter impacting China, Korea, Japan, and surrounding regions [*Chang and Lau*, 1982; *Ding and Krishnamurti*, 1987; *Jhun and Lee*, 2004], variability of winter temperature in East Asia and its causes have been investigated extensively. *Yang and Wu* [2013] revealed that the interdecadal variation in winter surface air temperature (SAT) over East Asia takes on two dominant modes, which can explain more than 60% of the total variance. One is a sign-consistent SAT variation, and the other depicts a meridional dipole structure between the northern and southern parts of East Asia. A similar spatial distribution can be found for winter SAT over China [*Kang et al.*, 2009]. Extreme weather in winter over East Asia is usually associated with severe SAT anomalies. For example, severe cold surges and snowstorms attacked South China in January 2008 and resulted in huge economic loss and severe social impacts. Thus, understanding the causes for the variability of East Asian winter SAT is crucial for climate prediction and human adaptation.

[3] One of the main factors contributing to winter SAT anomalies over East Asia is the East Asian winter monsoon (EAWM), which is one of the most conspicuous climate systems found in the Northern Hemisphere during boreal winter. When the EAWM is stronger (weaker) than normal, the northerly winds along coastal East Asia are more intense (moderate) and bring more (less) cold air to the Asian continent, leading to colder (milder) winters in East Asia [*Boyle and Chen*, 1987; *Chang et al.*, 2006; *Li and Wang*, 2012, 2013a, 2013b]. Accordingly, there has been much research effort devoted to understanding and predicting the EAWM. For example, its variation has been shown to be closely related to the expansion and shrinkage of the Siberian High [*Wu and Wang*, 2002; *Kim and Ahn*, 2012], which has been attributed to the strong radiative cooling induced by Eurasian continental snow cover during winter [*Watanabe and Nitta*, 1999; *Jeong et al.*, 2011]. When the Siberian High develops,

[1]Nansen-Zhu International Research Centre, Institute of Atmospheric Physics, Chinese Academy of Sciences, Beijing, China.
[2]Climate Change Research Center, Chinese Academy of Sciences, Beijing, China.
[3]University of Chinese Academy of Sciences, Beijing, China.

Corresponding author: S. He, University of Chinese Academy of Sciences, Beijing 100049, China. (hshp@mail.iap.ac.cn)

2169-897X/13/10.1002/2013JD020525

the northwesterly flow along the eastern flank of the Siberian High is enhanced and often brings severe cold surges and heavy snowfall events to East Asia [*Jhun and Lee*, 2004; *Li and Yang*, 2010]. Meanwhile, the variability of the Siberian High is closely related to the Arctic Oscillation (AO, also known as the Northern Hemisphere annular mode), proposed by *Thompson and Wallace* [1998]. *Wu and Huang* [1999] noted that the positive phase of the AO is favorable for a weakened Siberian High and EAWM. Furthermore, a significant out-of-phase relationship between the AO and EAWM was revealed by *Gong et al*. [2001], who suggested that the Siberian High might be a key system connecting the AO and the EAWM. By contrast, *Wu and Wang* [2002] argued that the winter AO can directly influence the EAWM-related circulation rather than through its impact on the Siberian High. Besides, the variability of the Aleutian Low, which can contribute to the west-east sea level pressure gradient favorable for the establishment of the EAWM, is closely related to the AO [*Overland et al*., 1999; *Sun and Wang*, 2006]. It has been found that the out-of-phase AO-EAWM relationship can be interpreted from the perspective of quasi-stationary planetary waves [*Thompson and Wallace*, 2000; *Chen and Huang*, 2002; *Chen et al*., 2005].

[4] At the same time, factors emanating from the tropical regions that influence the interannual variability of winter SAT over East Asia have also drawn much attention. *Wang* [2006] suggested that the El Niño-Southern Oscillation (ENSO) could influence winter SAT over East Asia through its impact on the EAWM. As revealed by *Li* [1990], severe cold wave activities frequently occur in East Asia prior to the occurrence of El Niño events. Besides, the EAWM is weaker than normal during El Niño winters because the convective activities over the western equatorial Pacific are suppressed and a southerly wind anomaly therefore appears along coastal East Asia [*Zhang et al*., 1996; *Zhang et al*., 1997]. *Wang et al*. [2000] pointed out that ENSO influences the EAWM through a Pacific-East Asian teleconnection. Climate model results have also provided evidence for the impact of tropical anomalies in the central and eastern Pacific on the interannual variability of East Asian winter SAT [*Ji and Sun*, 1997; *Gollan et al*., 2012]. However, the connection between ENSO and the EAWM is not stationary. *Zhou et al*. [2007] documented that the relationship between EAWM variability and ENSO on the interdecadal time scale undergoes low-frequency oscillation. Recently, it has been revealed that the interannual relationship between ENSO and the EAWM also takes on a low-frequency oscillation and weakened around the mid-1970s [*Wang and He*, 2012; *He and Wang*, 2013; *He et al*., 2013].

[5] Despite ENSO still being the most predictable climatic signal [*Kirtman and Schopf*, 1998; *Cheng et al*., 2011; *Sun and Wang*, 2012], the instability in the relationship between ENSO and other climatic systems might present greater challenges for climate prediction, and this means that we should pay more attention to the extratropical signals that could influence the climate. Actually, the potential climatic impacts of decreasing Arctic sea ice have been attracting increased attention [*Holland et al*., 2006; *Serreze et al*., 2007; *Wang and Overland*, 2009]. *Liu et al*. [2012] demonstrated that the decrease in autumn Arctic sea ice provides enhanced moisture sources for heavy snowfall in Europe during early winter and the northeastern and midwestern United States during winter. Owing to its significant impacts on atmospheric circulation through regional or large-scale radiative budgets, snow cover has been widely considered as an important predictor of winter climate [*Cohen and Saito*, 2003; *Fletcher et al*., 2007]. For instance, *Shabbar and Zhao* [2012] found that the late spring and early summer Eurasian snow-cover-extent anomaly is a skillful predictor of the following winter temperature anomalies over Canada. Besides, many previous studies have revealed that extratropical sea surface temperature (SST) variability can exert an impact on the mid-latitude climate through air-sea interactions [*Kushnir et al*., 2002; *Liu et al*., 2006; *Alexander and England*, 2007].

[6] Despite the above mentioned work, little attention has been paid to examining the potential influence of the preceding AO on the winter climate over East Asia. A recent study by *Kim and Ahn* [2012] revealed a possible influence of the November AO on East Asian winter temperature. According to *Kim and Ahn* [2012], when the November AO is in its positive (negative) phase, the intensity of the Siberian High weakens (strengthens), and the EAWM is therefore weakened (strengthened), leading to a warmer (colder) than normal winter in East Asia. Motivated by *Kim and Ahn* [2012], we found that the correlation of the November AO (Nov AO) is more significant with the East Asian temperature of the following January than that of the following December or February, which is discussed later in the paper. We further found that the December AO (Dec AO) is consistently highly correlated with the East Asian temperature of the following January. Effort is also made to understand the mechanisms of this influence of the Nov and Dec AO on the East Asian temperature of the following January.

2. Data and Methods

[7] The large-scale atmospheric data sets used in this study include monthly mean sea level pressure (SLP), winds at 850 hPa (uv850), winds at 1000 hPa (uv1000), geopotential height at 500 hPa (GPH500), 300 hPa zonal wind (u300), surface air temperature (SAT), and latent and sensible heat flux, derived from the National Centers for Environment Prediction/National Center for Atmospheric Research (NCEP/NCAR) reanalysis data set [*Kalnay et al*., 1996]. To support the results derived from NCEP/NCAR, SAT from the European Center for Medium-Range Weather Forecasts' 40 year Reanalysis (ERA40 [*Uppala et al*., 2005]) is employed. Monthly mean SST data are provided by the National Oceanic and Atmospheric Administration (NOAA); that is, the Extended Reconstructed version 3 SST analysis (1854–2012) [*Smith et al*., 2008].

[8] Monthly mean AO indices were obtained from the Climate Prediction Center (CPC) from their website at http://www.cpc.ncep.noaa.gov/products/precip/CWlink/daily_ao_index/ao.shtml. The Niño-3.4 index is defined as the area-weighted average SST anomalies (SSTAs) in the Niño-3.4 region (5°S–5°N, 170°–120°W). An East Asian temperature index (T_{EA}) is defined as the area-weighted mean surface air temperature in the domain (30°–45°N, 110°–150°E).

[9] In order to remove the possible linear impacts of ENSO when discussing the possible mechanism by which the Nov and Dec AO influence the East Asian temperature of the following January, we first performed a linear regression of the

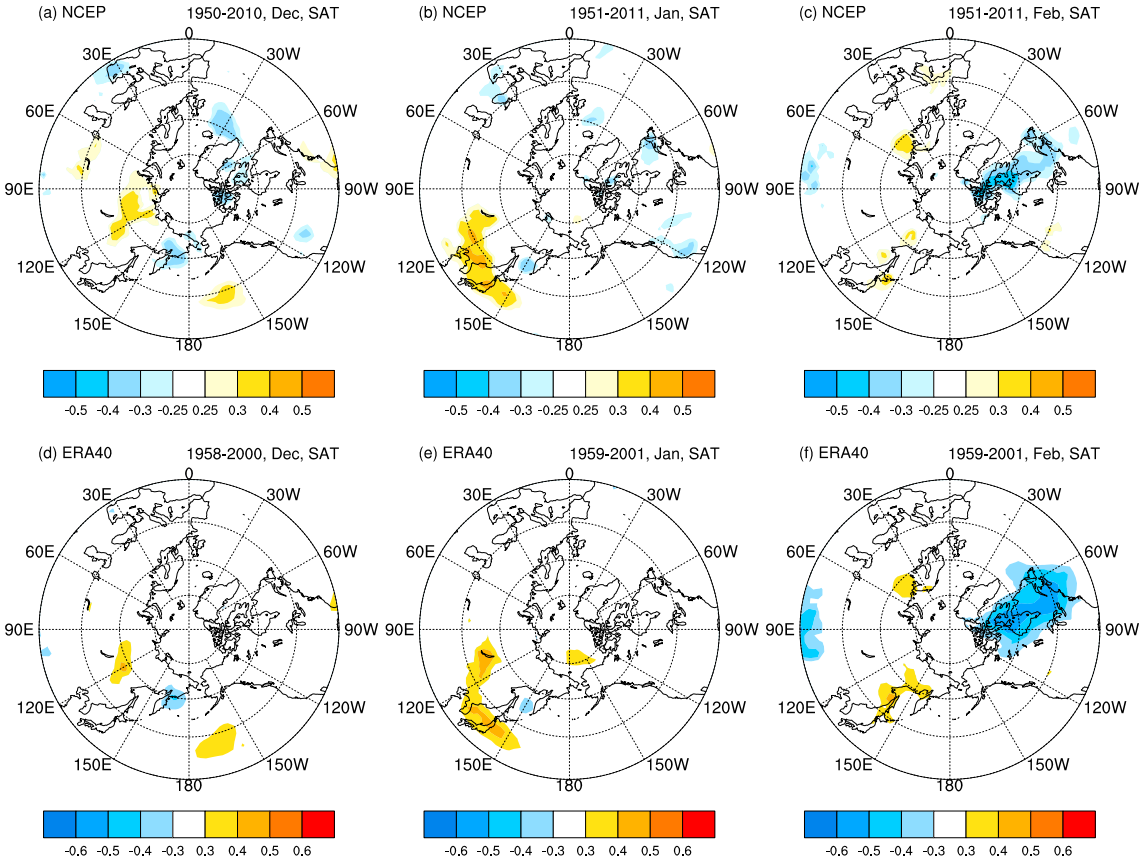

Figure 1. Correlation between Nov AO index and Northern Hemisphere SAT of the following December–January derived from NCEP/NCAR data during (a) December 1950–2010, (b) January 1951–2011, and (c) February 1951–2011. (d, e, and f) Same as Figures 1a, 1b, and 1c, respectively, but for the SAT derived from ERA40 data during December 1958–2000 (Figure 1d), January 1959–2001 (Figure 1e), and February 1959–2001 (Figure 1f). Shaded values are significant at the 95% confidence level based on the Student's *t* test.

variable with regard to simultaneous Niño-3.4 index and then obtained the residual variable from the difference between the original variable and the regressed one. To emphasize the interannual variability, we removed the linear trend for the aforementioned data.

3. Influence of the Nov and Dec AO on the East Asian Temperature of the Following January

[10] To determine which month in winter is affected most by the Nov AO, we first calculated the correlation of the Nov AO index with the following December, January, and February SAT anomalies (Figure 1). Interestingly, the Nov AO is not consistently highly correlated with each month's temperature. In December, there are few significant correlation coefficients in the Northern Hemisphere (Figure 1a). Significant values are mainly registered at high latitudes, such as northern Siberia and the Norwegian Sea. In contrast, significant positive correlation appears over central Siberia, North China, South Korea, and Japan in January (Figure 1b). The spatial distribution of correlation coefficients in January resembles the relationship between the Nov AO and East Asian winter temperature revealed by *Kim and Ahn* [2012]. Nevertheless, the significant positive correlation over East Asia disappears in February; instead, a significant negative correlation appears over northeastern North America (Figure 1c). To validate the above results derived from NCEP/NCAR data, we repeated the analysis using ERA40 SAT data, which is displayed in Figures 1d–1f and closely resembles the NCEP/NCAR-based results (Figure 1a versus 1d; Figure 1e versus 1b; Figure 1f

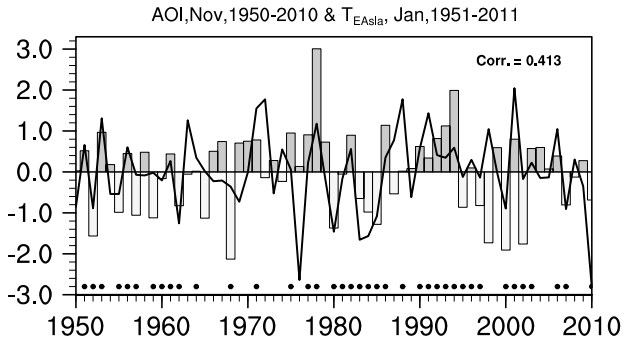

Figure 2. The normalized detrended time series of Nov AO index (AOI, bars) during 1950–2010, January SAT index over East Asia (30°–45°N, 110°–150°E, T_{EA}: line) during 1951–2011. The dots indicate those years when AOI and T_{EA} were in-phase. The correlation coefficient between the AOI and T_{EA} is given in the top right-hand corner.

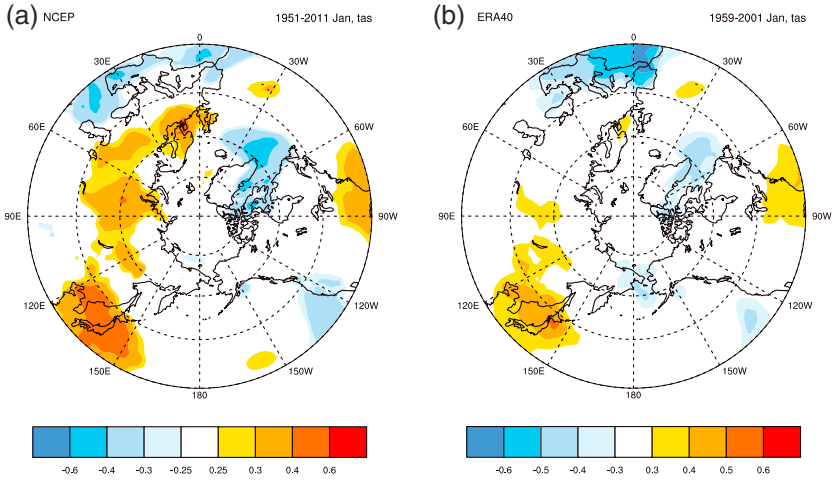

Figure 3. Correlation between Dec AO index and Northern Hemisphere SAT of the following January derived from (a) NCEP/NCAR data during 1951–2011 and (b) ERA40 data during 1959–2001. Shaded values are significant at the 95% confidence level based on the Student's *t* test.

versus 1c). Overall, Figure 1 confirms the fact that the impacts of the Nov AO on the East Asian temperature of the following January are more significant than those on the following December and February. Meanwhile, Figure 2 reveals the consistently in-phase variations of the time series between the Nov AO and the following January T_{EA}, with a correlation coefficient of 0.41 (99% confidence level). Moreover, 39 out of 61 years saw the Nov AO and the following January T_{EA} to be in-phase, which is about 64% of total events. Consequently, the following analysis will focus mainly on the January climate over East Asia.

[11] Another question we want to address is the following: Can the Dec AO influence the following January T_{EA}? Figure 3a illustrates the correlation between the Dec AO index and the following January's SAT anomalies. Surprisingly, based on the NCEP/NCAR reanalysis data, the January SAT associated with the Dec AO index shows considerably significant positive anomalies over Europe, Siberia, and East Asia. Furthermore, the spatial distribution of the correlation, especially in East Asia, derived from ERA40 SAT anomalies (Figure 3b), is in good agreement with the NCEP/NCAR-based results. A strongly significant correlation coefficient of 0.46 was also found between the Dec AO index and the following January T_{EA}, indicating a frequently in-phase relationship during the period 1950–2011 (Figure 4). There are 41 years when the Dec AO and the following January T_{EA} are in-phase, which accounts for about 67% of total events.

[12] To better understand the influence of the Nov and Dec AO on the East Asian temperature of the following January, a clear interpretation of the atmospheric circulation anomalies corresponding to the AO is required. For this purpose, we produced composite maps of the January EAWM-related circulation anomalies between high and low Nov/Dec AO events, based on a standard deviation of 0.5. Since the positive and negative phases of the composites largely mirror each other, our description and discussion in the following focuses mainly on the positive phase of the AO.

[13] In response to the positive Nov AO, significant negative and positive SLP anomalies form over Siberia and the North Pacific in January, respectively (Figure 5a, contours), suggesting a weakening of the Siberian High and Aleutian Low. Correspondingly, an anomalous surface cyclone and anticyclone appear over Siberia and the North Pacific, causing significant southerly wind anomalies to occur along coastal East Asia (Figure 5a, vectors). At 500 hPa (Figure 5b), significant positive anomalies extend from East Asia to the North Pacific, and negative anomalies are located in Siberia, implying the possibility that the January Ural High and East Asian Trough weaken when the preceding Nov AO is stronger than normal. Associated with the weakening of the Siberian High, the East Asian jet stream in its core region becomes weaker, and the zonal wind speed in the south and north of the core region gets stronger (Figure 5c). This means that the meridional shear of the East Asian jet stream is weakened, which gives rise to a weaker-than-normal EAWM [*Jhun and Lee*, 2004; *Li and Yang*, 2010; *He and Wang*, 2012]. In this sense, the preceding Nov AO exerts considerable impacts on the temperature of the following January over East Asia (Figure 5d) through its direct or indirect control of the following January's EAWM-related atmospheric circulation over the East Asia-North Pacific region.

[14] The influence of the Dec AO on the following January T_{EA} was also investigated in terms of the EAWM-related

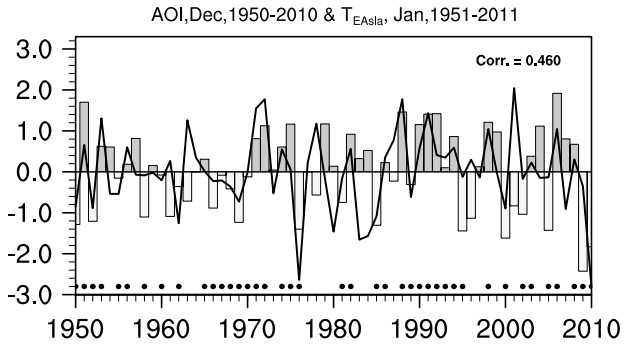

Figure 4. The normalized detrended time series of Dec AO index (AOI, bars) during 1950–2010 and January T_{EA} (line) during 1951–2011. The dots indicate those years when AOI and T_{EA} were in-phase. The correlation coefficient between the AOI and T_{EA} is given in the top right-hand corner.

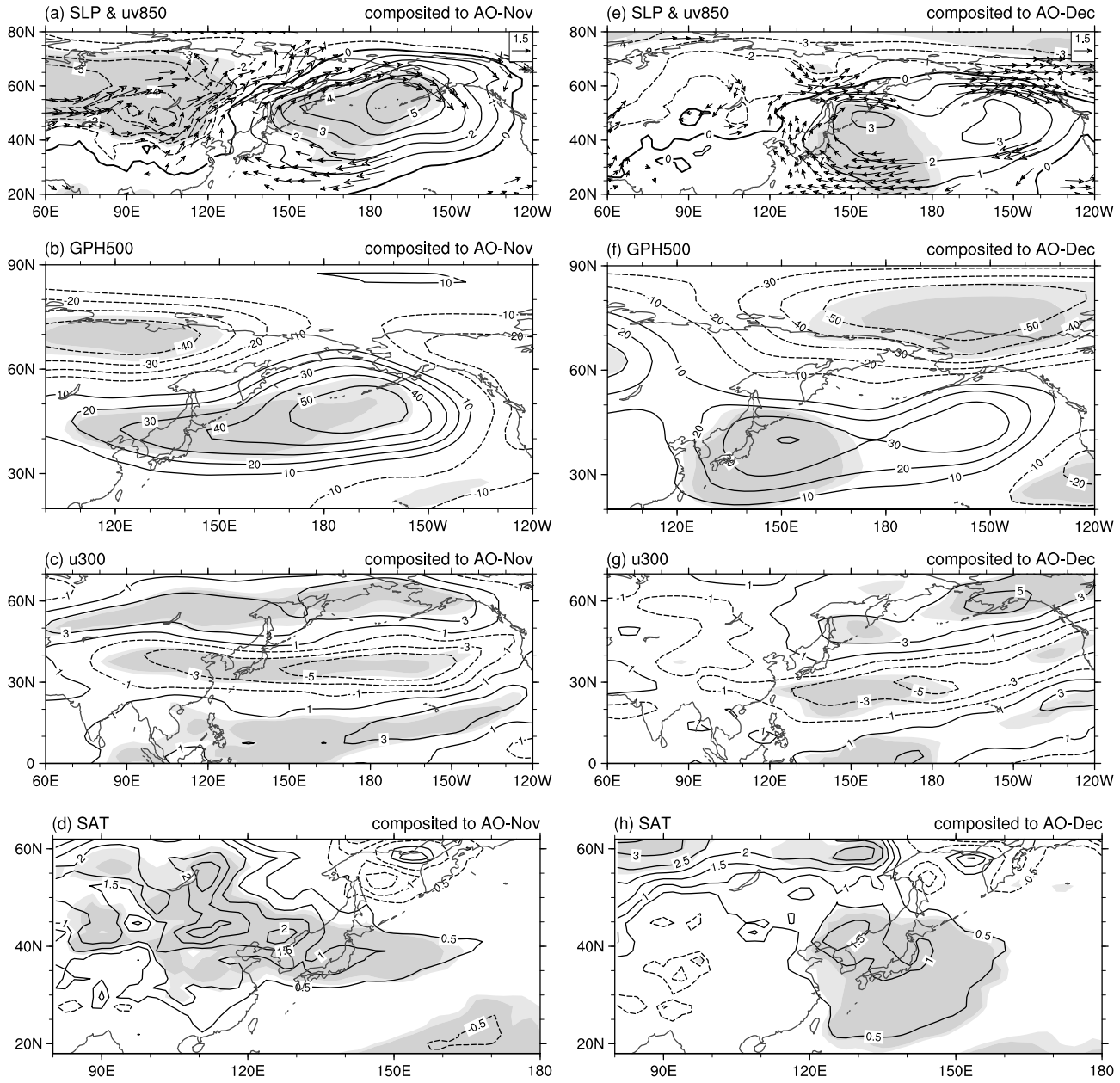

Figure 5. Composite maps of following January (a) 850 hPa wind (vectors) and SLP (shading), (b) 500 hPa geopotential height, (c) 300 hPa zonal wind, and (d) SAT anomalies between high and low Nov AO index years during 1950–2010. (e–h) Same as Figures 5a–5d but for the Dec AO index. The vector winds and shaded regions are significant at the 90% confidence level based on the Student's *t* test.

atmospheric circulation anomalies corresponding to the AO. As shown in Figures 5e–5f, the composites for the Dec AO are similar to those for the Nov AO but nevertheless display some differences. First, the SLP anomalies take on a south-north dipolar pattern from the midlatitudes to high latitudes, which resembles the positive phase of the AO (Figure 5e, contours). Second, significant positive and negative 500 hPa geopotential height anomalies are located in Japan and the Beaufort Sea, respectively (Figure 5f), which are northeast-southwest oriented and somewhat similar to the North Pacific Oscillation teleconnection [*Wallace and Gutzler*, 1981; *Linkin and Nigam*, 2008]. Third, even though there is a weakening of meridional shear of the East Asian jet stream (Figure 5g), the significant anomalies are mainly registered over the North Pacific. Nonetheless, the spatial pattern of atmospheric circulation anomalies in January connected with the preceding Dec AO still confirms the potential in-phase relationship between the Dec AO and the following January T_{EA}. This speculation is supported further by the significant positive January SAT anomalies around Japan following the positive phase of the Dec AO (Figure 5h).

[15] When taking into account both the November and December AO (Nov–Dec AO), the impacts of the preceding AO on the following January T_{EA} are much more significant. As illustrated by Figure 6, there are 46 out of 61 years when the Nov–Dec AO index and the following January T_{EA} are

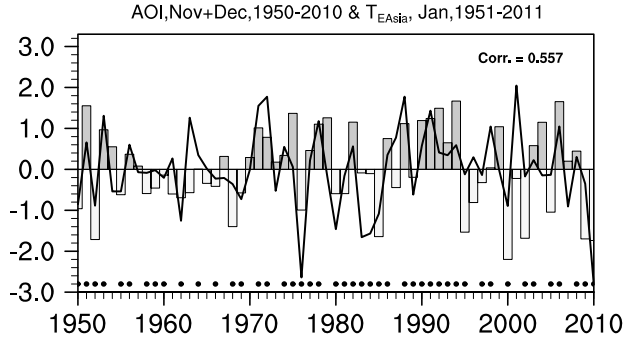

Figure 6. The normalized detrended time series of November and December mean AO index (AOI, bars) during 1950–2010 and January T_{EA} (line) during 1951–2011. The dots indicate those years when AOI and T_{EA} were in-phase. The correlation coefficient between the AOI and T_{EA} is given in the top right-hand corner.

in-phase. The frequency of in-phase occurrence is as high as 75%. Furthermore, the correlation coefficient between the Nov–Dec AO index and January T_{EA} is 0.56, which is statistically significant at the 99% confidence level. More details emerge from mapping the January atmospheric circulation anomalies onto the preceding Nov–Dec AO index (Figure 7). Following the stronger-than-normal AO events in November–December, during January, both the Siberian High and Aleutian Low are weakened significantly, leading to a weakening of the west-east and south-north SLP gradient, which is favorable for southerly wind anomalies along coastal East Asia (Figure 7a). Meanwhile, the East Asian jet stream over southern Japan weakens and the zonal wind speed in its south and north strengthens (Figure 7c). In this situation, the development of the East Asian Trough is usually suppressed [*Holton*, 1992]. Cold surges invading East Asia are fewer than normal, and a warm climate ensues (Figure 7d).

4. Possible Mechanisms

[16] To examine how the Nov/Dec AO influences the following January T_{EA}, we first need to gain insight into the evolution of the atmospheric circulation associated with the Nov/Dec AO. Figures 8 and 9 illustrate the regressed map of SLP and GPH500 anomalies with regard to Nov/Dec AO index, respectively. In terms of large-scale atmospheric circulation, the SLP/GPH500 anomalies related to the Nov AO (Figures 8a–8c and 9a–9c) appear to be maintained into the following 2 months, with negative and positive anomalies located in the high and low latitudes, respectively, which resemble the positive phase of the AO. The spatial correlation coefficients between the regressed SLP/GPH500 anomalies in November with regard to simultaneous AO index and those in the following December (January) to the preceding Nov AO index are 0.57(0.63)/0.46(0.63). However, the correlation coefficient between Nov AO index and the following December (January) AO index is 0.22 (0.24), which is barely statistically significant at the 90% confidence level (Table 1). This implies that, besides the weak persistence of the Nov AO-related atmospheric circulation, there should be another mechanism by which the Nov AO influences the following January T_{EA}, which will be discussed below. From the perspective of regional circulation, we can see a clear development of the EAWM-related circulation following the Nov AO. In November, significant positive SLP anomalies extend eastward from west of Baikal to the North Pacific, and negative anomalies are mainly confined to the Arctic (Figure 8a). In the following 2 months, the negative signals over western Russia gradually move southeastward over time from December to January. In January, the negative anomalies over Siberia expand toward the south and are further reinforced (Figure 8c). Furthermore, the positive anomalies over the East Asian continent (Figures 8a and 8b) weaken and expand eastward. Positive anomalies eventually prevail and are reinforced over the North Pacific in January. The Siberian High and Aleutian Low are therefore weakened significantly in January following a positive-phase Nov AO event. Such evolution of SLP anomalies associated with the Nov AO indicates an eastward propagation of AO signals, which might be attributed to the stationary Rossby wave. This is evident by inspecting Figures 9a–9c, which display the GPH500 anomalies from November to January regressed to Nov AO index. The spatial distribution of GPH500 anomalies in November mainly resembles the positive phase of AO pattern. Over the Eastern Hemisphere, the positive anomalies center in the eastern Atlantic, negative anomalies center in Europe, and positive anomalies over Baikal comprise a wave pattern that starts from the eastern Atlantic and extends eastward (Figure 9a). This wave pattern can be better recognized from the midtroposphere streamfuction anomaly fields (not shown). In December, the alternative occurrence of the "positive"-"negative"-"positive" anomalies pattern can still be observed over Eurasia. However, the wave pattern is mainly dominant over high latitudes (north of 45°N, Figure 9b). Consequently, significant positive SAT anomalies only appear over the north of Siberia in December after a stronger-than-normal Nov AO event (Figures 1a and 1d). In the following January, the "positive" and "negative" anomaly centers located in the eastern Atlantic and Europe remain evident. However, the "positive" anomaly center located in Siberia is pushed aside by negative anomalies and eventually moves southeastward to East Asia (Figure 9c). This implies that the Rossby wave shifts southward, and the signals of the preceding Nov AO could therefore be transmitted to East Asia in January. This southward shift is more dominant in the midtroposphere streamfuction anomaly fields (not shown). Such a hypothesis might be supported by Figures 10a–10c, which show the regression of November–January 500 hPa quasi-geostrophy streamfunction (QGSF: contours) and wave activity flux (WAF: vectors) computed according to Plumb's formulation [*Plumb*, 1985] with regard to Nov AO index. As we know, the WAF describes the propagation of stationary Rossby waves. Associated with a positive-phase Nov AO event, an eastward propagation of Rossby wave is visible over high latitudes of Eurasia (Figure 10a). This Rossby wave appears to persist into the following December and remains dominant over high latitudes (Figure 10b). It should be noted that another wave source region in eastern Asia, which was revealed by the work of *Yang and Gutowski* [1994], shows up and might contribute to the weakening of the East Asian Trough. By January, the anomalous wave activities over central Siberia move southeastward to East Asia, which is consistent with the results in the previous analysis. Hence, the impact of the Nov AO could be transmitted to the following January T_{EA}.

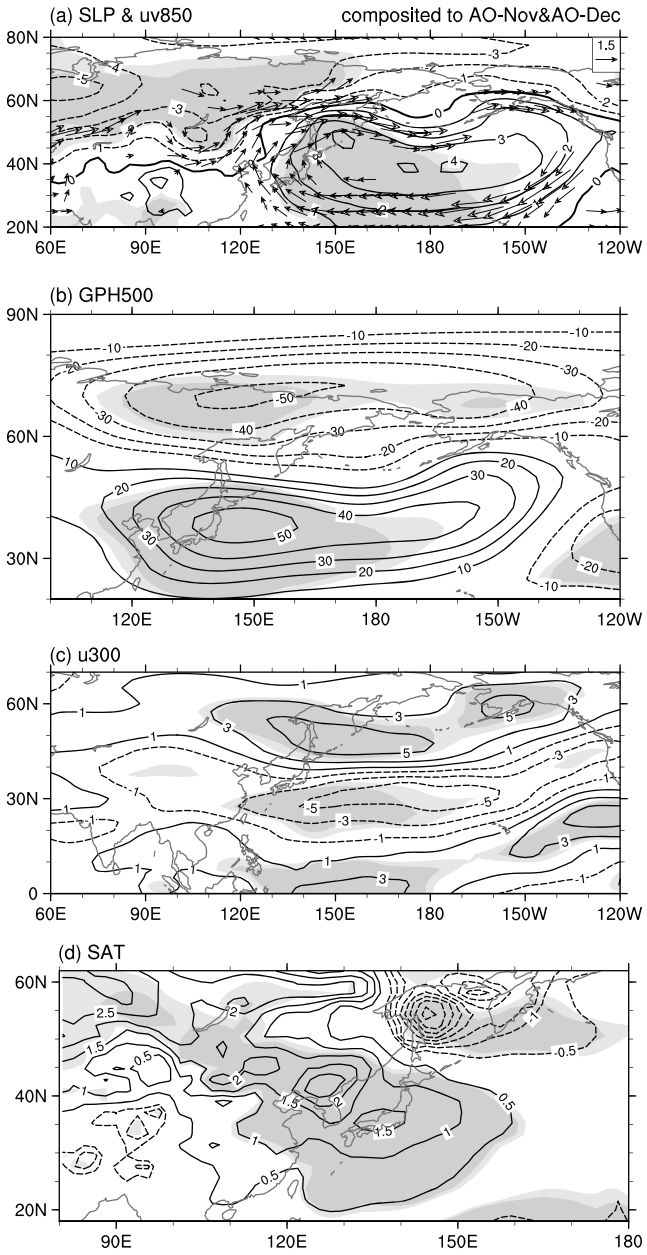

Figure 7. The same as Figure 5, but for anomalies composited to November and December mean AO index.

[17] Meanwhile, the large-scale atmospheric circulation anomalies related to the Dec AO (Figures 8d, 8e, 9d, and 9e) seem to persist well into the following January. The spatial correlation coefficient between the regressed SLP/GPH500 anomalies in December with regard to simultaneous AO index and those in the following January to the preceding Dec AO index is 0.87/0.86. The resemblance can be confirmed by the correlation coefficient between the Dec AO index and the following January AO (Jan AO) index, which is as high as 0.46 and significant at the 99% confidence level (Table 1). To better reflect this persistence, in Figures 10d and 10e we display the regression of December–January 500 hPa QGSF (contours) and WAF (vectors) with regard to Dec AO index. Accompanying the positive-phase Dec AO event, a wave pattern starts from the eastern Atlantic and propagates southeastward to Europe. Then, this wave pattern bifurcates into two branches, with one extending eastward and poleward to the north of Baikal and the other turning southeastward to East Asia (Figure 10d). By the following January, these two wave branches remain evident. However, it is important to note that a new wave source region emerges over East Asia and emits an eastward propagation of wave activity (Figure 10e). This wave momentum would weaken the East Asian Trough, leading to a weaker-than-normal EAWM in January. As a result, the SAT in January over East Asia is usually warmer when the preceding Dec AO is stronger than normal, and vice versa.

[18] According to *Wang et al*. [2000], the atmosphere alone cannot provide a long-term memory because of the chaotic nature of the atmospheric motion. Thus, the aforementioned impacts of Nov/Dec AO-related atmospheric anomalies might also be maintained by local atmosphere-ocean interaction. To examine the role of air-sea interaction

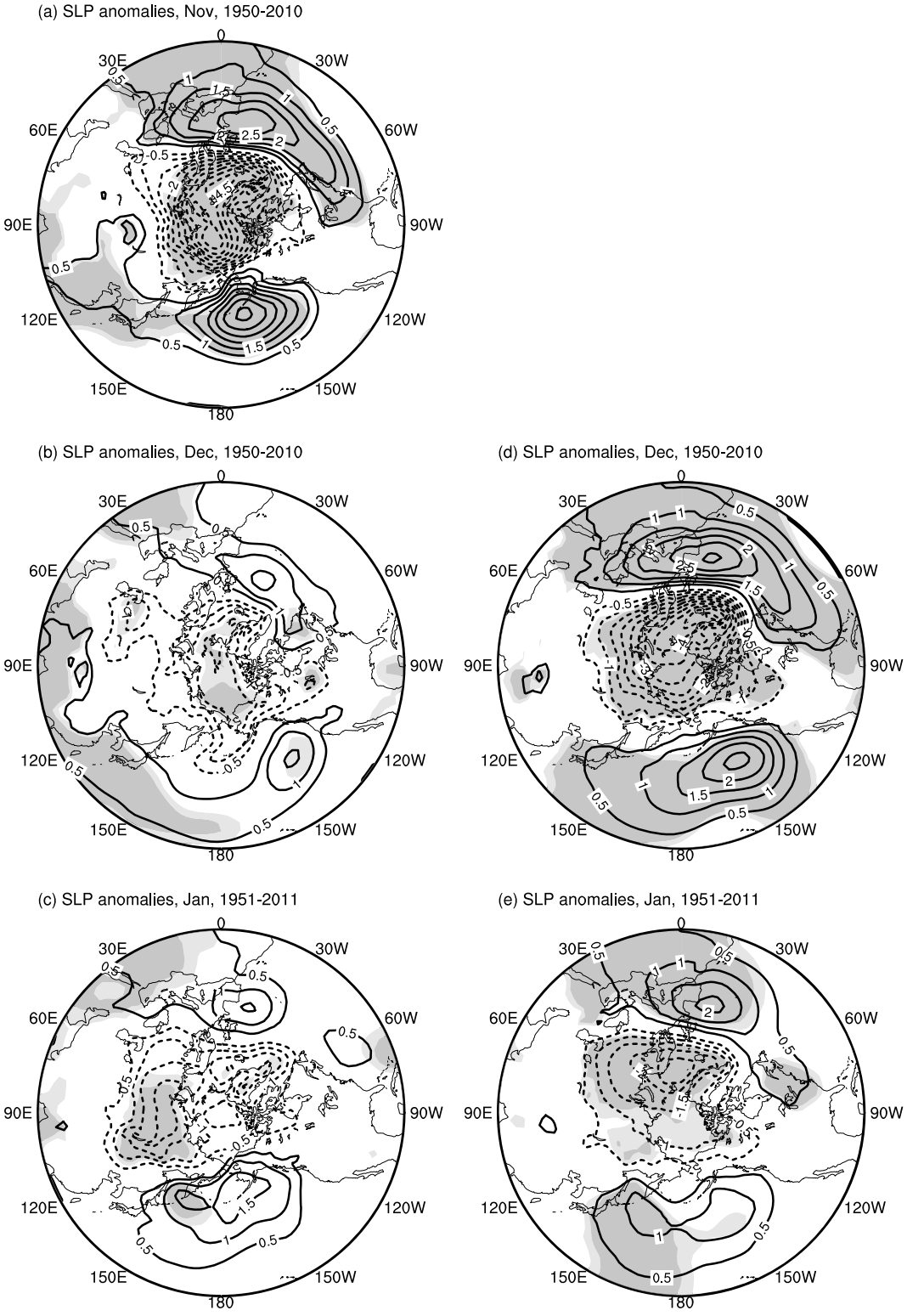

Figure 8. Regression maps of (a) November, (b) December, and (c) following January SLP anomalies with regard to Nov AO index during 1950–2010. (d and e) Same as Figures 8b and 8c, respectively, but with regard to Dec AO index during 1950–2010. Light and dark shaded values are significant at the 90% and 95% confidence levels based on the Student's *t* test.

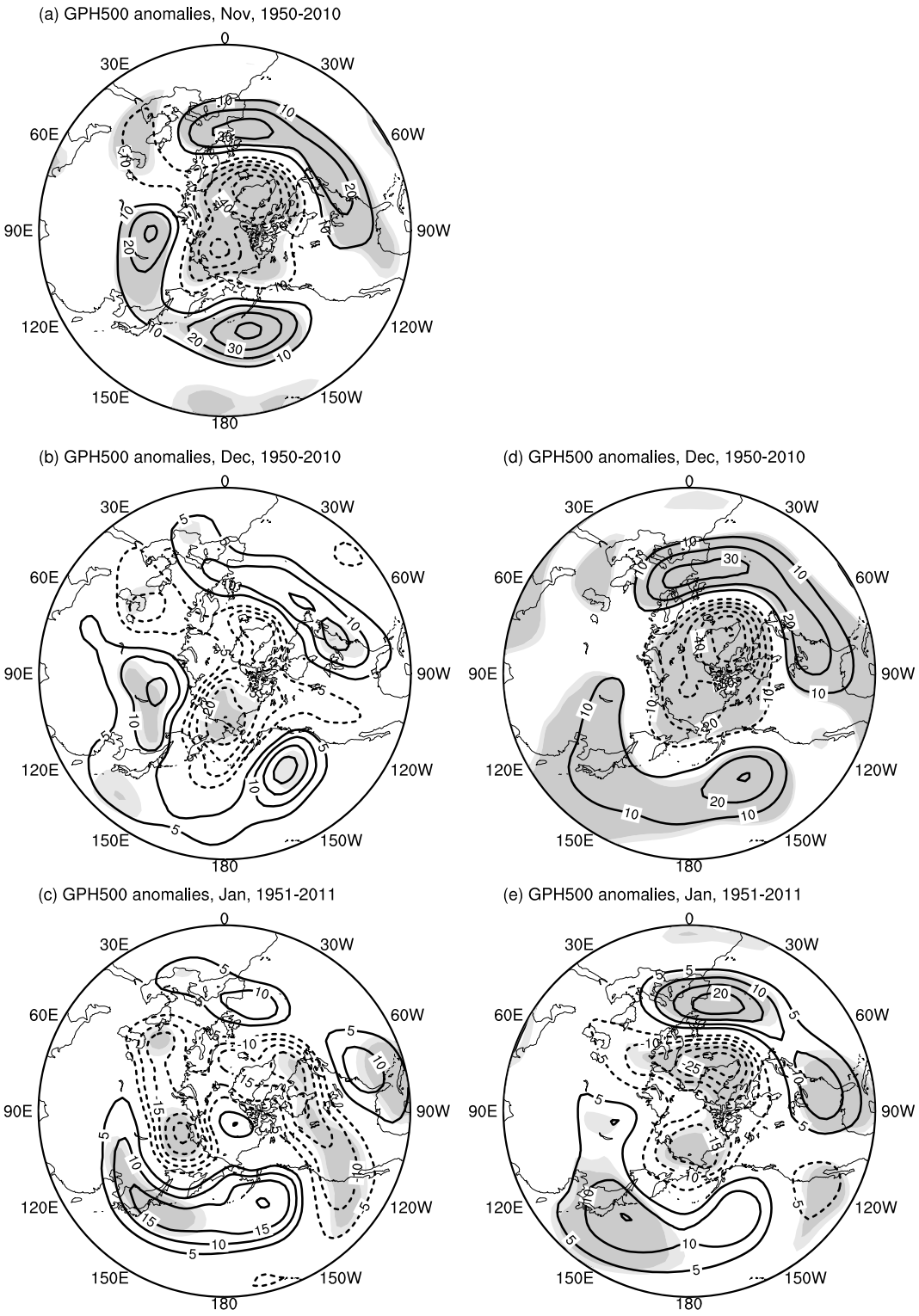

Figure 9. The same as Figure 8 but for the 500 hPa geopotential height anomalies.

over the North Pacific in transmitting the Nov/Dec AO signals into the following January, we further illustrate the evolution of the SST, 1000 hPa wind, and turbulent heat flux anomalies associated with the Nov/Dec AO in Figure 11. In November, a significant anomalous anticyclone occupies the North Pacific when the simultaneous AO is stronger than normal (Figure 11a, vectors). Correspondingly, anomalous northwesterly winds prevail along the western coast of Canada and northeasterly winds flow from the California coast to the western subtropical North Pacific, which bring cold horizontal advection to these maritime regions. Thus, anomalous surface heat flux from the ocean to the atmosphere takes place where colder-than-normal SSTAs therefore occur. Meanwhile, southeasterly winds blow westward and poleward

Table 1. Correlation Coefficients Between Different Indices During 1950–2010/1951–2011[a]

	AO Nov	AO Dec	AO Jan	I_{SSTA1} Jan	I_{SSTA2} Jan
AO Nov					
AO Dec	*0.22*				
AO Jan	*0.24*	**0.46**			
I_{SSTA1} Jan	*0.22*	**0.34**	**0.31**		
I_{SSTA2} Jan	−0.19	**−0.46**	**−0.31**	**−0.54**	
I_{SSTA3} Jan	*0.21*	**0.37**	**0.29**	**0.65**	**−0.80**

[a]The italic and bold values exceed the 90% and 95% confidence levels according to the Student's *t* test, respectively.

to the central subtropical North Pacific (around 40°N, 180°) where warm horizontal advection prevails, making the ocean obtain surface heat flux from the atmosphere and causing warming SSTAs to occur in this region. In this sense, such a pattern of SSTAs in the North Pacific is forced to form by the atmospheric anomalies associated with the Nov AO, which is supported theoretically by *Davis* [1976] and *Miller et al.* [1994], who suggested that the midlatitude atmospheric circulation anomalies act as a forcing factor to drive the variation in extratropical SSTAs. The pattern of SSTAs persists into the following December and keeps on developing due to the anomalous anticyclone located in the eastern subtropical North Pacific (Figure 11b). The negative SSTAs located in the west of California in particular become more significant, and the SSTAs over the Bering Sea change from positive conditions into negative ones. As a result, a horseshoe SSTA, which was first revealed by *Liu et al.* [2006], preliminarily takes shape. By January, the horseshoe SSTAs are eventually mature, with significant positive SSTAs located in the central subtropical North Pacific (around 40°N, 160°W), surrounded by significant negative SSTAs (Figure 11c). Analogously, an anomalous anticyclone over the North Pacific related to the simultaneous Dec AO appears to contribute to the formation of horseshoe SSTAs (Figure 11d), which could also persist into the following January and become more significant and

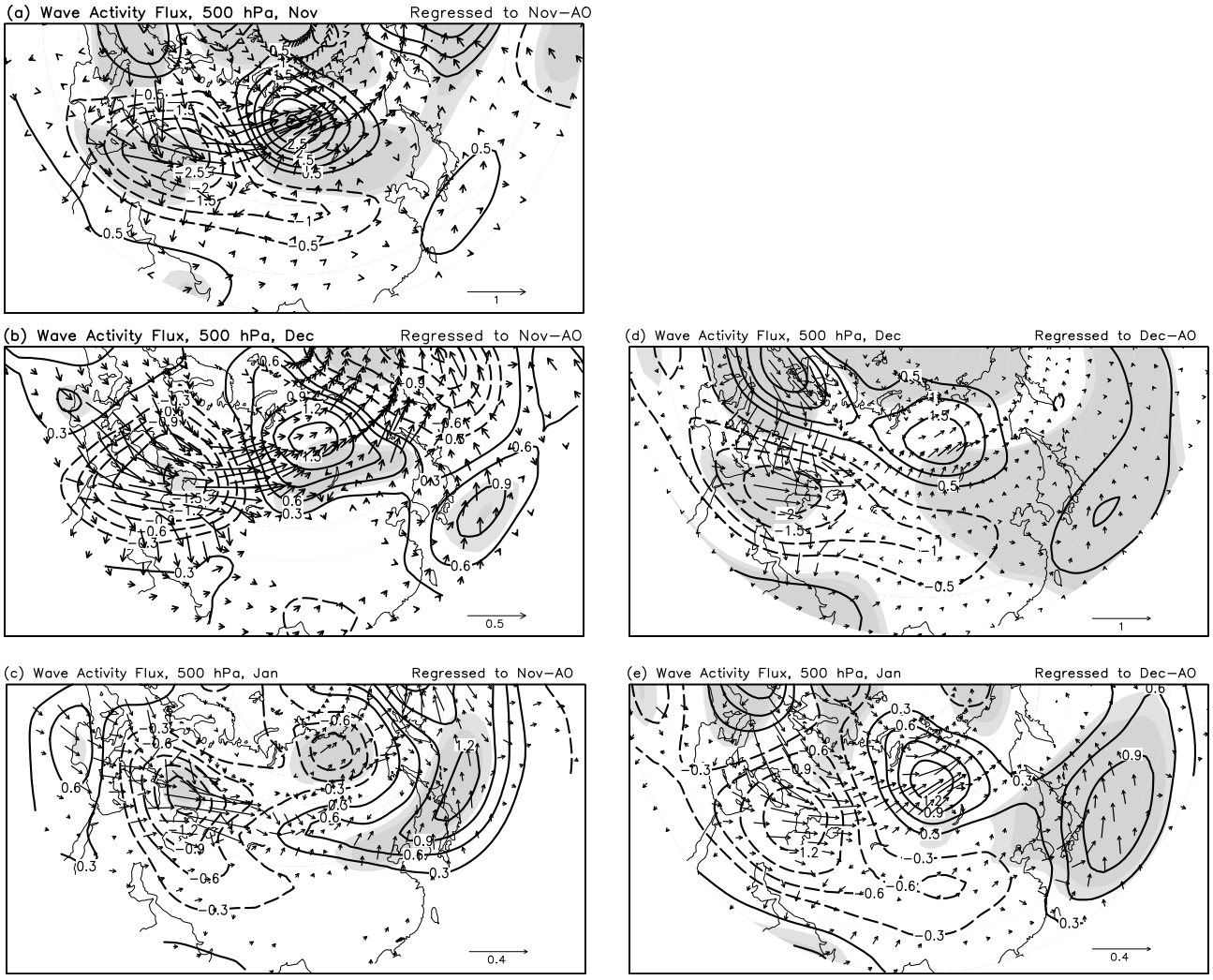

Figure 10. Regression maps of the 500 hPa quasi-geostrophy streamfunction (contours: $10^6\ m^2\ s^{-1}$) and wave activity flux (vectors: scale in $m^2\ s^{-2}$) in (a) November, (b) December, and (c) the following January with regard to Nov AO index during 1950–2010. (d and e) Same as Figures 10b and 10c, respectively, but with regard to Dec AO index during 1950–2010. Light and dark shaded values are significant at the 90% and 95% confidence levels based on the Student's *t* test.

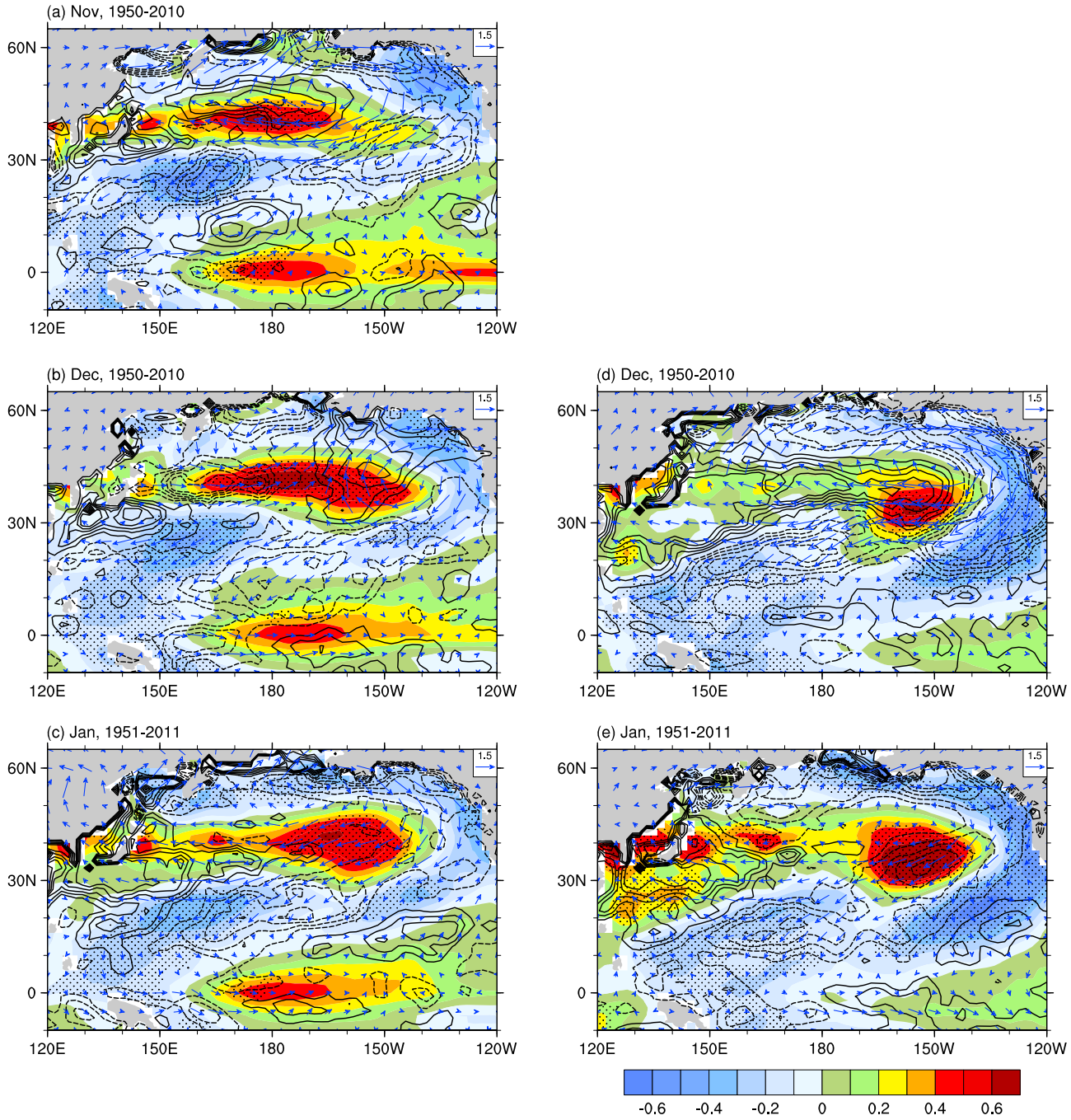

Figure 11. Composite maps of the (a) November, (b) December, and (c) following January 1000 hPa wind (vectors: m s^{-1}), sea surface temperature (shading: °C), and turbulent heat flux (contours: latent plus sensible, W m^{-2}) anomalies between high and low Nov AO index years during 1950–2010. (d and e) Same as Figures 11b and 11c, respectively, but with regard to Dec AO index during 1950–2010. Positive/negative heat flux values are solid/dashed contours every 3, and the zero contour is ignored. The SST enclosed by the dotted regions and the vector winds are significant at the 90% confidence level based on the Student's *t* test.

well-developed (Figure 11e). It should be noted that the surface wind anomalies over the central subtropical North Pacific change suddenly from southerly to northerly anomalies in the following January (Figures 11c and 11e). At the same time, the turbulent heat flux anomalies in this region change from positive to negative, implying that the horseshoe SSTAs begin to impact the local atmosphere. Locally, the in situ warming in the central subtropical North Pacific and cooling in the west coast of North America could effectively stimulate an anomalous anticyclone to occur over the North Pacific by strengthening the northern temperature gradient and weakening the southern one.

[19] Based on the above analysis, we suggest that the horseshoe SSTAs in January are related to the former Nov/Dec AO and act as a forcing factor of the simultaneous atmosphere. To determine the potential relationship between the North Pacific

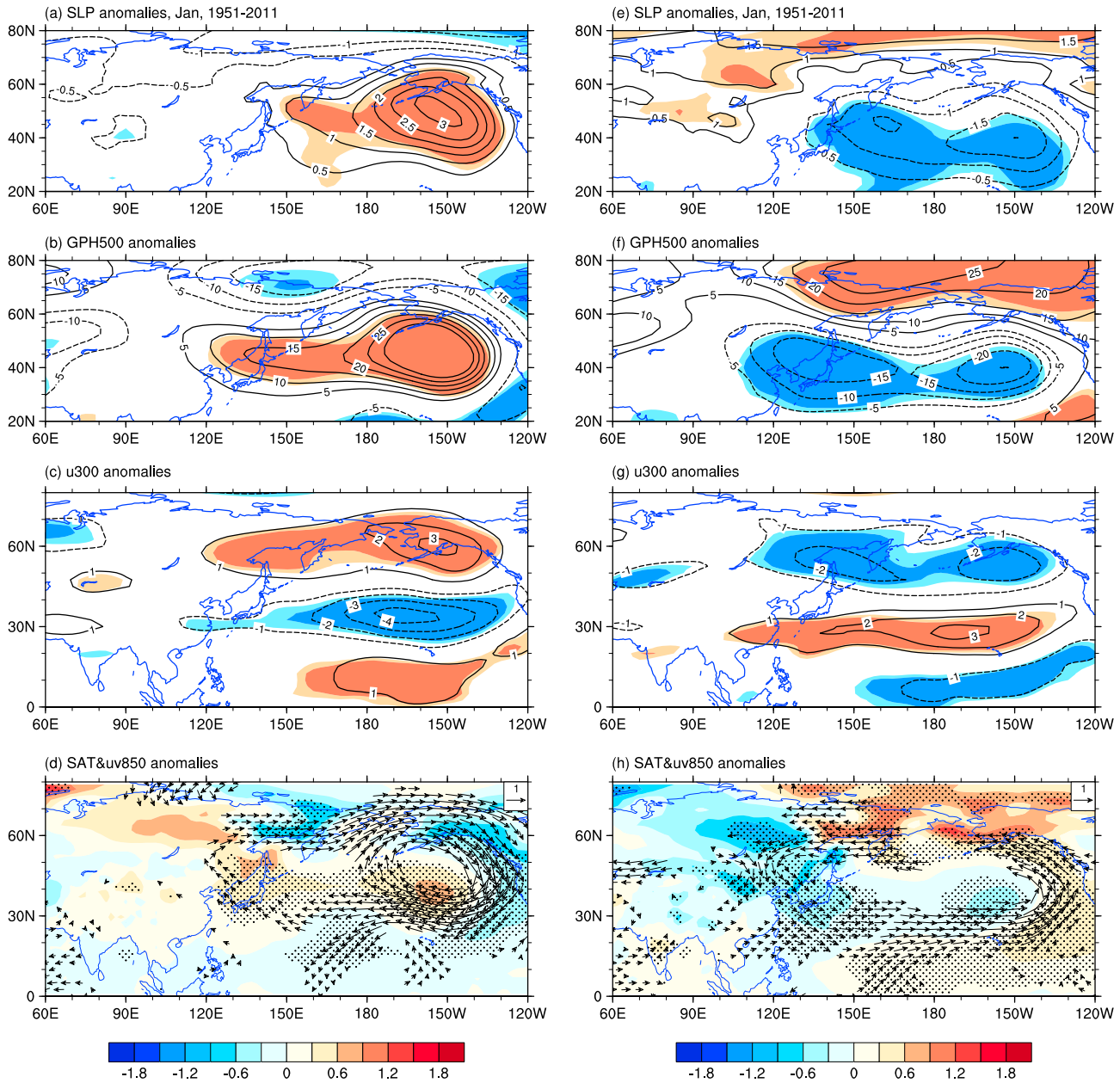

Figure 12. Regression maps of (a, e) January SLP, (b, f) 500 hPa geopotential height, (c, g) 300 hPa zonal wind, and (d, h) SAT and 850 hPa wind anomalies with regard to January SSTAs area-averaged in (Figures 12a–12d) significant positive regions of Figure 11e over the central northeastern North Pacific (20°–50°N, 180°–120°W, I_{SSTA1}) and (Figures 12e–12h) significant negative regions of Figure 11e over the coastal eastern North Pacific (10°–70°N, 180°–120°W, I_{SSTA2}) during 1951–2011. Light and dark shaded values in Figures 12a–12c and 12e–12g are significant at the 90% and 95% confidence level based on the Student's *t* test. The SAT enclosed by the dotted regions and the vector winds in Figures 12d and 12h are significant at the 90% confidence level based on the Student's *t* test.

SSTAs and EAWM-related atmospheric anomalies, we defined three SSTA indices for the North Pacific. The domains are confined to the significant positive regions of Figure 11e over the central subtropical North Pacific (20°–50°N, 180–120°W, region A) and significant negative regions in Figure 11e over the coastal eastern North Pacific (10°–70°N, 180–120°W, region B). The normalized area-weighted average SSTAs in regions A and B are denoted as I_{SSTA1} and I_{SSTA2}, respectively, and the horseshoe SSTA index is defined as I_{SSTA1} minus I_{SSTA2}, denoted as I_{SSTA3}. Since the anomalies in the central and eastern tropical Pacific are barely significant (Figure 11), the ENSO effect was removed for the following analysis by excluding the linear regression with regard to simultaneous Niño-3.4 index. Figure 12 illustrates the January regression maps with regard to simultaneous I_{SSTA1} (Figures 12a–12d) and I_{SSTA2} (Figures 12e–12h). It can be seen that the linkage of the atmospheric anomalies with the SSTAs in regions A and B is much more dominant at

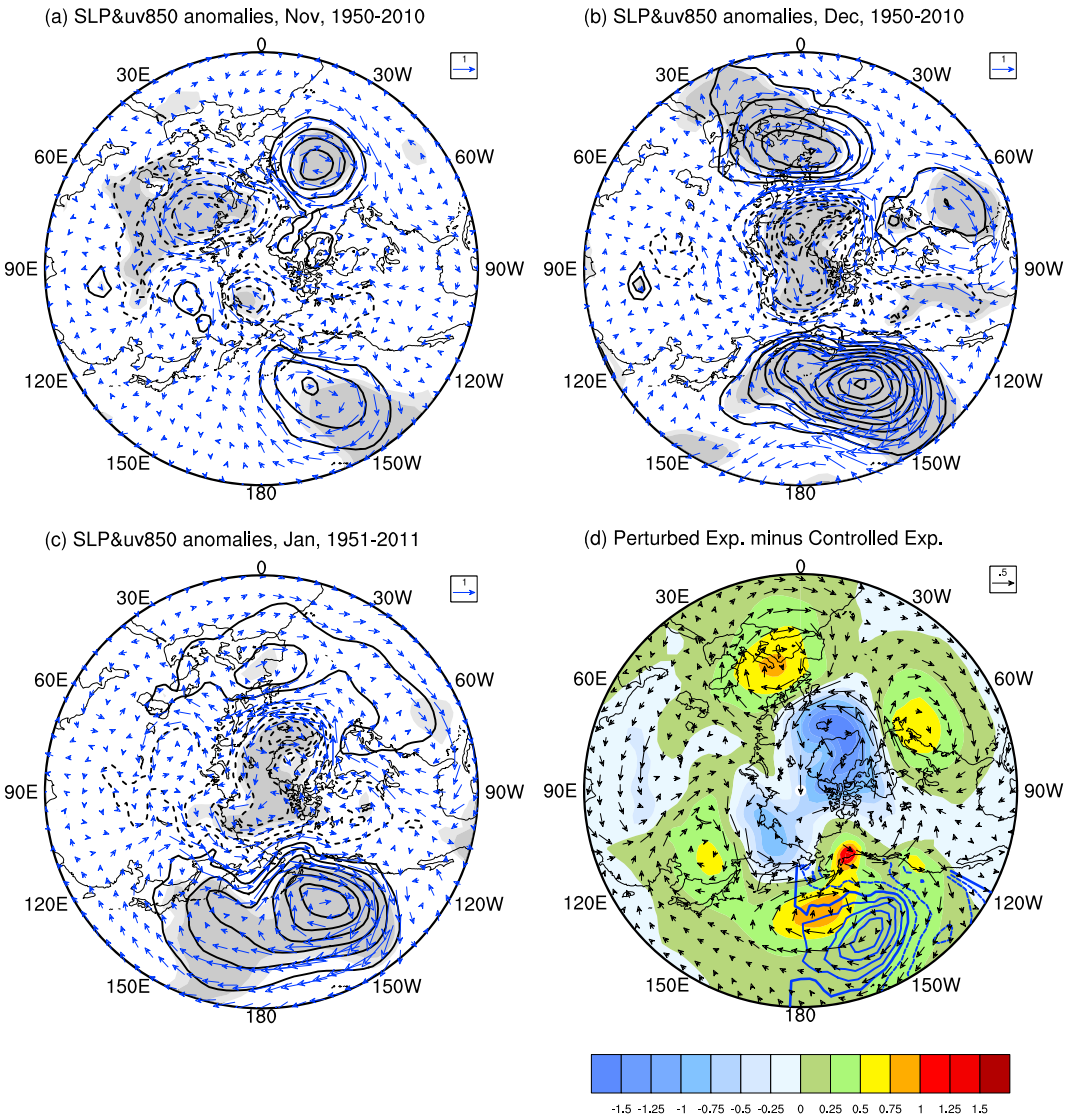

Figure 13. Regression of the SLP (contours, interval of 0.5 hPa, zero lines ignored) and 850 hPa wind (vectors) anomalies for (a) the preceding November, (b) December, and (c) January with regard to January I_{SSTA3} during 1951–2011. Light and dark shaded regions indicate that the anomalies are significant at the 90% and 95% confidence levels based on the Student's t test. (d) Difference of SLP (shaded) and 850 hPa wind (vectors) between the perturbed experiment forced by January horseshoe SSTAs (i.e., January mean plus the horseshoe SSTAs shown as blue contours, interval of 0.2°C) and the control experiment simulated by the NCAR Community Atmosphere Model version 3.1.

midlatitudes and high latitudes. When the SSTAs in region A are significantly warmer, significant positive anomalies are observed in the SLP and GPH500 field over the North Pacific (Figures 12a and 12b). Furthermore, the 300 hPa zonal wind anomalies show three significant "positive," "negative," and "positive" bands located from the low latitudes, midlatitudes, and high latitudes, respectively (Figure 12c). Accordingly, an anomalous anticyclone emerges in the North Pacific, which yields significant southeasterly anomalies and warming conditions over East Asia (Figure 12d). In other words, warming SSTAs in region A are conducive to a weakening of the EAWM-related circulation. The SSTAs in region B show similar but opposite and more significant correlation with the EAWM-related circulation, relative to the SSTAs in region A (Figures 12e–12h).

[20] The above identified local atmospheric response to the North Pacific regional SSTAs implies possible significant impacts of the horseshoe SSTAs on the EAWM-related circulation. From the point of view of dynamics, we propose that a positive feedback mechanism plays a critical role between horseshoe SSTAs and atmospheric circulation in the North Pacific. The November/December anomalous anticyclone over the North Pacific related to simultaneous positive-phase AO could induce warming in the central subtropical North Pacific and cooling along the west coast of North America. These Nov AO-related SSTAs could persist into the following 2 months, developing in December and maturing in January. In addition, the Dec AO-related SSTAs in the North Pacific also show evident maintenance and are well-developed in the following January. The connection of the January

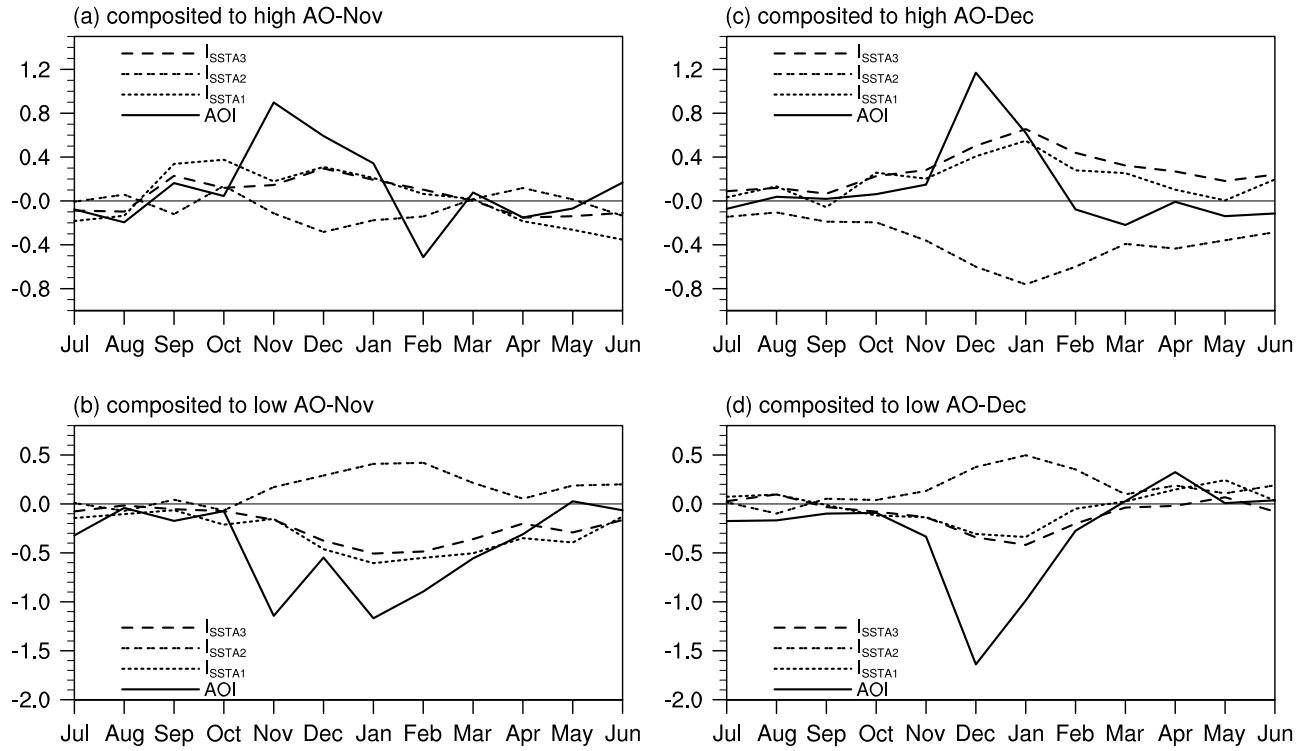

Figure 14. Monthly mean AO index (AOI), I_{SSTA1}, I_{SSTA2}, and I_{SSTA3} for the (a) high Nov AO years and (b) low Nov AO years. (c and d) Same as Figures 14a and 14b, respectively, but for high and low Dec AO years.

horseshoe SSTAs with the preceding Nov/Dec AO is clearly illustrated by Figures 13a–13c, which display the November-January regressed SLP (contours) and 850 hPa wind (vectors) anomalies with regard to January I_{SSTA3}. Before the January horseshoe SSTAs form, the November SLP field shows significant negative anomalies over continental Europe and dominant positive ones over the North Atlantic and North Pacific. The two anomalous anticyclones located in the North Pacific and North Atlantic, together with an anomalous cyclone over the Arctic, imply the potential effect of the Nov AO in the formation of the January horseshoe SSTAs (Figure 13a). The spatial distribution of the SLP anomalies in the preceding December is characterized by a primary negative center over the Arctic and significant positive fluctuations located in the North Atlantic and North Pacific. It displays a more zonal symmetric appearance and resembles the AO pattern (Figure 13b). Interestingly, the spatial distribution of the January SLP anomalies resembles the AO pattern as well (Figure 13c), but the signals are relatively weaker than those in the preceding December. This feature suggests that the formation of the January horseshoe SSTAs is likely attributable to the preceding AO. Such speculation can be confirmed by the significant correlation coefficient (0.21/0.46, Table 1) between the preceding Nov/Dec AO index and January I_{SSTA3}.

[21] To better reflect the evolution of the horseshoe SSTAs associated with the Nov and Dec AO, we present in Figure 14 the evolution of monthly mean AO index, I_{SSTA1}, I_{SSTA2}, and I_{SSTA3} for high and low November years (Figures 14a and 14b, respectively) and high and low Dec AO years (Figures 14c and 14d, respectively). For convenience, we focus on the major negative phase of AO episodes (Figures 14b and 14d), although the figures also include the major positive phase of AO episodes (i.e., Figures 14a and 14c). One of the conspicuous features is that the rapid drop (rise) of SST over the central subtropical North Pacific (west coast of North America) often occurs a month later when the Nov/Dec AO is significantly weaker than normal. Following the negative phase of the Nov AO, the December I_{SSTA1}/I_{SSTA2} keeps on dropping/rising and peaks in the following January. Therefore, the establishment of the horseshoe SSTAs generally lags the anomalous Nov (Dec) AO by 2 months (1 month) (Figures 14c and 14d). This is consistent with the scenario described in Figure 11. However, the well-developed horseshoe SSTAs rapidly collapse in February. The evolution revealed in Figure 14 satisfactorily explains why the Nov AO impacts the following January T_{EA} by skipping December T_{EA} and why the influence of the Nov/Dec AO disappears in February and thereafter.

[22] When the horseshoe SSTA is well established in January, the air temperature over the North Pacific exhibits a similar pattern, with a warming center located in the central subtropical North Pacific around (40°N, 160°W) and surrounded by cooling anomalies (Figure 15d, shading). Furthermore, the amplitudes of the boundary temperature anomalies are comparable to those of the ocean, suggesting the existence of highly effective turbulent mixing in the boundary layer. In this sense, the horseshoe SSTAs on the one hand increase the northern meridional temperature gradient and on the other hand reduce the southern one. Based on thermal wind theory [*Holton*, 1992], the westerly wind strengthens in the north and weakens in the south. Consequently, a huge anomalous anticyclone occurs over the North Pacific (Figure 15d) and is accompanied by a weakened Siberian High and Aleutian Low (Figure 15a).

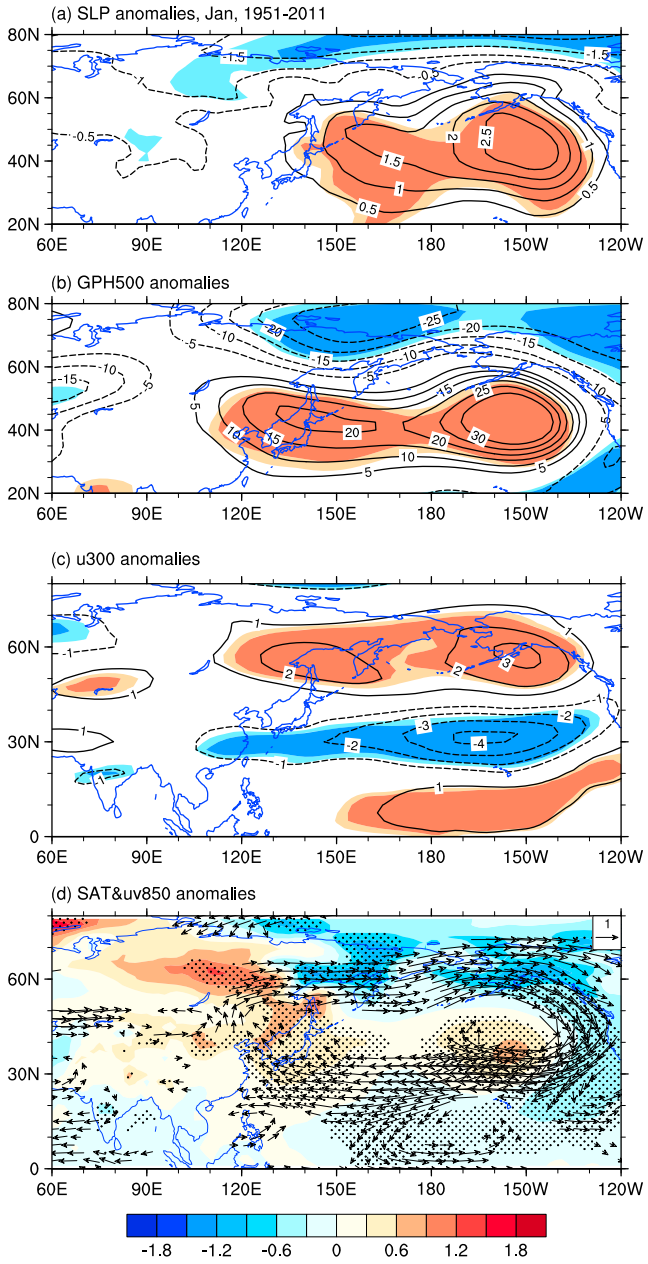

Figure 15. The same as Figures 12a–12d, respectively, but with regard to the horseshoe SSTAs index.

Consistent with the anomalies in the boundary layer, a weakened Ural High and East Asian Trough appear in the middle troposphere (Figure 15b). In the 300 hPa zonal wind field, significant negative anomalies are located in the regions where the East Asian jet stream core is located, including South China and the southern part of Japan [*Yang et al.*, 2002]. Meanwhile, the zonal winds both in the north and south of the jet stream become strong (Figure 15c). Such a "positive-negative-positive" anomalies pattern in the upper tropospheric zonal wind would favor a situation in which the East Asian Trough is shallow, the Siberian High and Aleutian Low are weak, and low-level southerly wind anomalies prevail over East Asia [*Li and Yang*, 2010]. As a result, the SAT over East Asia is warmer than normal (Figure 15d). Therefore, the positive feedback between the anomalous anticyclonic wind and horseshoe SSTAs in the North Pacific may play an important role in the development and maintenance of the EAWM-related atmospheric anomalies.

[23] To assess the contribution of the January horseshoe SSTAs to the formation of the weaker-than-normal EAWM, we used the NCAR Community Atmospheric Model Version 3.1 (CAM3.1) [*Collins et al.*, 2006] to perform two simple experiments. The control experiment was integrated with a given climatological SST distribution. In the perturbed experiment, the January horseshoe SSTAs in the domain (10°–70°N, 180°–120°W), as shown in Figure 11e (shading) and indicated by the blue contours in Figure 13d, were added to the mean SST over the North Pacific. Total SST was then used as lower-boundary forcing. The resultant anomalous SLP and 850 hPa wind were obtained by subtracting the climatology of the control experiment from the long-term mean simulation of the perturbed experiment. The spatial distribution of simulated SLP anomalies (Figure 13d, shading) displays qualitative similarities with the observed counterparts (Figure 13c, contours). The most important feature to note is the anomalous southerly wind prevailing over East Asia (Figure 13d, vectors). This means that the EAWM is relatively weak when a horseshoe SSTA appears over the North Pacific. Even though the simulated atmospheric anomalies are weaker than their observed counterparts, the results shown in Figure 13d imply that the horseshoe SSTAs are partially responsible for the formation of the North Pacific anomalous anticyclone, which leads to a weaker-than-normal EAWM.

5. Summary and Discussion

[24] In this study we investigated the nonsimultaneous coefficient between the preceding AO and winter T_{EA}. The results derived from both NCEP/NCAR and ERA40 reanalysis data indicated that the correlation of the Nov AO with the following January T_{EA} is much more significant than that with the following December and February T_{EA} (Figure 1). In addition, we found that the Dec AO also seems to influence the following January T_{EA} (Figure 3). The correlation coefficients of Nov AO and Dec AO index with the following January T_{EA} are 0.41 and 0.46, respectively, and both are significant at the 99% confidence level. This indicates a frequently in-phase occurrence between the preceding Nov/Dec AO and January T_{EA} during the period 1950–2011, which is supported by the fact that 39 (41) out of 61 years saw the Nov (Dec) AO and the following T_{EA} to be in-phase (Figures 2 and 4). Composite analysis revealed that, following a stronger-than-normal Nov AO event, the SLP field in January shows significant negative anomalies over Siberia and significant positive anomalies in the North Pacific, indicating an obvious weakening of the Siberian High and Aleutian Low. As a result, southeasterly wind anomalies appear along the west flank of the Aleutian Low and southwesterly wind anomalies are seen along the east flank of the Siberian High. This is opposite to the climatological anticyclonic circulation associated with the Siberian High pressure system, suggesting that the northerly wind is weaker and the cold air reaching East Asia is less than normal. Meanwhile, significant negative GPH500 anomalies are located in Siberia, and positive anomalies extend from North China to the North Pacific, implying a weakening of the Ural High and East Asian Trough. Besides, the 300 hPa zonal wind

displays three "positive-negative-positive" anomaly bands from the low latitudes, midlatitudes, and high latitudes over the East Asia-North Pacific region; the negative band is located in the domain (25°–40°N, 80°E–150°W), together with one positive band over (45°–65°N, 60°E–140°W) and the other positive band over (0°–20°N, 90°E–140°W). This three-band structure is closely connected to the weakening of low-level meridional northerly wind over East Asia. These atmospheric anomalies are favorable for a weaker-than-normal EAWM, and the January SAT over East Asia is therefore increased (Figures 5a–5d). Similarly, dominant atmospheric anomalies in January are observed in the East Asia-North Pacific region after a positive phase of the Dec AO (Figures 5f–5h). For instance, a weakened Aleutian Low causes southeasterly wind anomalies to occur along coastal East Asia, and the East Asian Trough is rather weaker. On the other hand, there are also some distinctions. For example, negative SLP anomalies are located in the Arctic rather than in Siberia, and negative GPH500 anomalies appear over the Arctic Ocean instead. These features make the atmospheric anomalies from the low levels to the middle troposphere to be north-south oriented rather than northwest-southeast oriented and resemble part of the positive phase of the AO. The 300 hPa zonal wind anomalies also display a three-band structure but are located more eastward. Consequently, the climate in January over North China, Korea, and Japan is warmer. When taking into account both the Nov and Dec AO (Nov–Dec AO), the impacts of the preceding AO on the following January atmospheric circulation over the East Asia-North Pacific are much more dominant. The correlation coefficient between the Nov–Dec AO index and the January T_{EA} is 0.56, which means that about 31% of the variance of January East Asian temperature could be accounted for by the preceding Nov and Dec AO (Figures 6 and 7).

[25] Evolution of the preceding Nov/Dec AO-related atmospheric anomalies reveals that the Nov/Dec AO pattern could persist, to some extent, into the following January. In terms of large-scale atmospheric circulation, the SLP/GPH500 anomalies related to the Nov or Dec AO appear to be maintain into the following January in the form of an AO signature (Figures 8 and 9). The spatial correlation coefficients between the regressed SLP/GPH500 anomalies in November (December) with regard to simultaneous Nov (Dec) AO index and those in the following January to the preceding Nov (Dec) AO index are 0.63(0.87)/0.63(0.86). Furthermore, the correlation coefficient between the Nov AO index and the following Dec (Jan) AO index is 0.22 (0.24), which is statistically significant at the 90% confidence level. Besides, the correlation coefficient between the Dec AO index and the following Jan AO index is as high as 0.46 and significant at the 99% confidence level (Table 1). We argue that the Nov/Dec AO exerts its impact on the following T_{EA} through a stationary Rossby wave. Accompanying the positive phase of the Nov AO, an eastward propagation of the wave occurs over Eurasia. These wave activities are still evident but remain dominant over the high latitudes in the following December. That is why few temperature anomalies are observed over East Asia in December. However, the anomalous wave activities over central Siberia move southeastward to East Asia, which makes the transmission of Nov AO signals into the following January T_{EA} possible (Figures 10a–10c). The December stationary Rossby wave associated with the simultaneous AO, which bifurcates into two branches, with one extending eastward and poleward to the north of Baikal and the other turning southeastward to East Asia, could also persist into the following January (Figures 10d and 10e). Consequently, the January T_{EA} could be significantly influenced by the preceding Dec AO.

[26] Considering the chaotic nature of the atmospheric motion, we also propose that an in situ positive feedback mechanism might play a critical role between the SSTAs and atmospheric circulation in the North Pacific. The positive-phase Nov/Dec AO could induce a horseshoe SSTA in the North Pacific, which is well developed and mature in the following January (Figure 11). This speculation is partially supported by the analogous AO signature in SLP anomalies for November/December regressed to the January horseshoe SSTA index (Figures 13a–13c) and is further confirmed by the time evolution, which reveals that the SST over the central subtropical North Pacific (west coast of North America) often rapidly rises (drops) a month later and peaks in the following January when the Nov/Dec AO is significantly stronger than normal (Figure 14). However, the well-developed horseshoe SSTAs rapidly collapse in February. The evolution revealed in Figure 14 satisfactorily answers why the Nov AO impacts on the following January T_{EA} by skipping December T_{EA} and why the influence of Nov/Dec AO disappears in February and thereafter.

[27] From the atmospheric perspective, such a horseshoe SSTA could lead to a strengthening of the air temperature gradient in the north and a weakening in the south due to effective turbulent mixing in the boundary layer. This implies that the westerly wind strengthens in the north and weakens in the south. A huge anomalous anticyclone therefore emerges in the North Pacific, causing anomalous southeasterly winds to occur along coastal East Asia. Concurrent with the anomalies in the boundary layer, a weakened Ural High and East Asian Trough appear in the middle troposphere, and significant negative anomalies emerge in the regions where the East Asian jet stream core is located. A weak EAWM therefore forms, and the SAT over East Asia is warmer than normal (Figure 15).

[28] The potential contribution of the horseshoe SSTA pattern to the formation of the North Pacific anticyclone anomaly was verified by experiments with CAM3.1. An AO pattern with an anomalous anticyclone over the North Pacific was simulated well, which displayed qualitative similarities with its observed counterpart (Figure 13d). However, the underestimated anomaly amplitude implies the requirement for a time-dependent calculation with a coupled atmosphere-ocean model to better understand the dynamics of the positive feedback mechanism proposed in this study. Moreover, other external factors, such as snow cover and sea ice, might be favorable for the persistent impacts of the Nov/Dec AO into the following January. Much more research is needed in this regard.

[29] **Acknowledgment.** This research was supported by the National Natural Science Foundation of China (grants 41210007 and 41130103).

References

Alexander, S., and M. H. England (2007), Coupled ocean-atmosphere feedback in the Southern Annular Mode, *J. Clim.*, *20*, 3677–3692, doi:10.1175/JCLI4200.1.

Boyle, J. S., and T. Chen (1987), Synoptic aspects of the wintertime East Asian monsoon, in *Monsoon Meteorology*, edited by C. P. Chang and T. N. Krishnamurti, pp. 125–160, Oxford Univ. Press, Oxford, U. K.

Chang, C., Z. Wang, and H. Hendon (2006), The Asian winter monsoon, in *The Asian Monsoon*, edited by B. Wang, pp. 89–127, Springer Press, Berlin, Heidelberg.

Chang, C. P., and K. M. Lau (1982), Short-term planetary-scale interactions over the tropics and mid-latitudes during northern winter. Part I: Contrasts between active and inactive periods, *Mon. Weather Rev.*, *110*, 933–946, doi:10.1175/1520-0493(1982)110<0933:STPSIO>2.0.CO;2.

Chen, W., and R. Huang (2002), The propagation and transport effect of planetary waves in the Northern Hemisphere winter, *Adv. Atmos. Sci.*, *19*, 1113–1126.

Chen, W., S. Yang, and R. Huang (2005), Relationship between stationary planetary wave activity and the East Asian winter monsoon, *J. Geophys. Res.*, *110*, D14110, doi:10.1029/2004JD005669.

Cheng, Y., Y. Tang, and D. Chen (2011), Relationship between predictability and forecast skill of ENSO on various time scales, *J. Geophys. Res.*, *116*, C12006, doi:10.1029/2011JC007249.

Cohen, J. L., and K. Saito (2003), Eurasian snow cover, more skillful in predicting US winter climate than the NAO/AO?, *Geophys. Res. Lett.*, *30*(23), 2190, doi:10.1029/2003GL018053.

Collins, W. D., et al. (2006), The formulation and atmospheric simulation of the Community Atmosphere Model Version 3 (CAM3), *J. Clim.*, *19*, 2144–2161.

Davis, R. E. (1976), Predictability of sea surface temperature and sea level pressure anomalies over the North Pacific Ocean, *J. Phys. Oceanogr.*, *6*, 249–266.

Ding, Y., and T. N. Krishnamurti (1987), Heat budget of the Siberian high and the winter monsoon, *Mon. Weather Rev.*, *115*, 2428–2449, doi:10.1175/1520-0493(1987)115<2428:HBOTSH>2.0.CO;2.

Fletcher, C. G., P. J. Kushner, and J. Cohen (2007), Stratospheric control of the extratropical circulation response to surface forcing, *Geophys. Res. Lett.*, *34*, L21802, doi:10.1029/2007GL031626.

Gollan, G., R. J. Greatbatch, and T. Jung (2012), Tropical impact on the East Asian winter monsoon, *Geophys. Res. Lett.*, *39*, L17801, doi:10.1029/2012GL052978.

Gong, D., S. Wang, and J. Zhu (2001), East Asian winter monsoon and Arctic oscillation, *Geophys. Res. Lett.*, *28*, 2073–2076, doi:10.1029/2000GL012311.

He, S., and H. Wang (2012), An integrated East Asian winter monsoon index and its interannual variability (in Chinese), *Chin. J. Atmos. Sci.*, *36*, 523–538.

He, S., and H. Wang (2013), Oscillating relationship between the East Asian winter monsoon and ENSO, *J. Clim.*, doi:10.1175/JCLI-D-13-00174.1.

He, S., H. Wang, and J. Liu (2013), Changes in the relationship between ENSO and Asia-Pacific mid-latitude winter atmospheric circulation, *J. Clim.*, *26*, 3377–3393, doi:10.1175/JCLI-D-12-00355.1.

Holland, M., C. Bitz, and B. Tremblay (2006), Future abrupt reductions in the summer Arctic sea ice, *Geophys. Res. Lett.*, *33*, L23503, doi:10.1029/2006GL028024.

Holton, J. R. (1992), *An Introduction to Dynamic Meteorology*, 3rd ed., 511 pp., Academic Press, MA, USA.

Jeong, J. H., T. Ou, H. W. Linderholm, B. M. Kim, S. J. Kim, J. S. Kug, and D. Chen (2011), Recent recovery of the Siberian High intensity, *J. Geophys. Res.*, *116*, D23102, doi:10.1029/2011JD015904.

Jhun, J. G., and E. J. Lee (2004), A new East Asian winter monsoon index and associated characteristics of the winter monsoon, *J. Clim.*, *17*(4), 711–726, doi:10.1175/1520-0442(2004)017<0711:ANEAWM>2.0.CO;2.

Ji, L., and S. Sun (1997), Model study on the interannual variability of Asian winter monsoon and its influence, *Adv. Atmos. Sci.*, *14*(1), 1–22.

Kalnay, E., M. Kanamitsu, R. Kistler, W. Collins, D. Deaven, L. Gandin, M. Iredell, S. Saha, G. White, and J. Woollen (1996), The NCEP/NCAR 40-year reanalysis project, *Bull. Am. Meteorol. Soc.*, *77*(3), 437–471, doi:10.1175/1520-0477(1996)077<0437:TNYRP>2.0.CO;2.

Kang, L., W. Chen, L. Wang, and L. Chen (2009), Interdecadal variations of winter temperature in China and their relationship with the atmospheric circulation and sea surface temperature (in Chinese), *Chin. J. Atmos. Sci.*, *14*(1), 45–53.

Kim, H.-J., and J.-B. Ahn (2012), Possible impact of the autumnal North Pacific SST and November AO on the East Asian winter temperature, *J. Geophys. Res.*, *117*, D12104, doi:10.1029/2012JD017527.

Kirtman, B. P., and P. S. Schopf (1998), Decadal variability in ENSO predictability and prediction, *J. Clim.*, *11*(11), 2804–2822, doi:10.1175/1520-0442(1998)011<2804:DVIEPA>2.0.CO;2.

Kushnir, Y., W. Robinson, I. Bladé, N. Hall, S. Peng, and R. Sutton (2002), Atmospheric GCM response to extratropical SST anomalies: Synthesis and evaluation*, *J. Clim.*, *15*(16), 2233–2256, doi:10.1175/1520-0442(2002)015<2233:AGRTES>2.0.CO;2.

Li, C. (1990), Interaction between anomalous winter monsoon in East Asia and El Nino events, *Adv. Atmos. Sci.*, *7*(1), 36–46.

Li, F., and H. Wang (2012), Predictability of the East Asian winter monsoon interannual variability as indicated by the DEMETER CGCMS, *Adv. Atmos. Sci.*, *29*, 441–454, doi:10.1007/s00376-011-1115-3.

Li, F., and H. Wang (2013a), Relationship between Bering Sea ice cover and East Asian winter monsoon year-to-year variations, *Adv. Atmos. Sci.*, *30*, 48–56, doi:10.1007/s00376-012-2071-2.

Li, F., and H. Wang (2013b), Autumn sea ice cover, winter Northern Hemisphere annular mode, and winter precipitation in Eurasia, *J. Clim.*, *26*, 3968–3981.

Li, Y., and S. Yang (2010), A dynamical index for the East Asian winter monsoon, *J. Clim.*, *23*(15), 4255–4262, doi:10.1175/2010JCLI3375.1.

Linkin, M. E., and S. Nigam (2008), The north pacific oscillation-west Pacific teleconnection pattern: Mature-phase structure and winter impacts, *J. Clim.*, *21*(9), 1979–1997, doi:10.1175/2007JCLI2048.1.

Liu, J., J. A. Curry, H. Wang, M. Song, and R. M. Horton (2012), Impact of declining Arctic sea ice on winter snowfall, *Proc. Natl. Acad. Sci.*, *109*, 6781–6783, doi:10.1073/pnas.1114910109.

Liu, Q., N. Wen, and Z. Liu (2006), An observational study of the impact of the North Pacific SST on the atmosphere, *Geophys. Res. Lett.*, *33*, L18611, doi:10.1029/2006GL026082.

Miller, A. J., D. R. Cayan, T. P. Barnett, N. E. Graham, and J. M. Oberhuber (1994), Interdecadal variability of the Pacific Ocean: Model response to observed heat flux and wind stress anomalies, *Clim. Dyn.*, *9*(6), 287–302, doi:10.1007/BF00204744.

Overland, J. E., J. M. Adams, and N. A. Bond (1999), Decadal variability of the Aleutian Low and its relation to high-latitude circulation*, *J. Clim.*, *12*(5), 1542–1548, doi:10.1175/1520-0442(1999)012<1542:DVOTAL>2.0.CO;2.

Plumb, R. A. (1985), On the three-dimensional propagation of stationary waves, *J. Atmos. Sci.*, *42*, 217–229.

Serreze, M., M. Holland, and J. Stroeve (2007), Perspectives on the Arctic's shrinking sea-ice cover, *Science*, *315*, 1533–1536, doi:10.1126/science.1139426.

Shabbar, A., and H. Zhao (2012), Contribution of late spring Eurasian snow cover extent to Canadian winter temperatures, *Int. J. Climatol.*, *32*(14), 2124–2133, doi:10.1002/joc.2426.

Smith, T. M., R. W. Reynolds, T. C. Peterson, and J. Lawrimore (2008), Improvements to NOAA's historical merged land-ocean surface temperature analysis (1880–2006), *J. Clim.*, *21*(10), 2283–2296, doi:10.1175/2007JCLI2100.1.

Sun, B., and H. Wang (2012), Larger variability, better predictability?, *Int. J. Climatol.*, doi:10.1002/joc.3582.

Sun, J., and H. Wang (2006), Relationship between Arctic oscillation and Pacific decadal oscillation on decadal timescale, *Chin. Sci. Bull.*, *51*(1), 75–79, doi:10.1007/s11434-004-0221-3.

Thompson, D. W. J., and J. M. Wallace (1998), The Arctic Oscillation signature in the wintertime geopotential height and temperature fields, *Geophys. Res. Lett.*, *25*(9), 1297–1300, doi:10.1029/98GL00950.

Thompson, D. W. J., and J. M. Wallace (2000), Annular modes in the extratropical circulation. Part I: Month-to-month variability*, *J. Clim.*, *13*(5), 1000–1016, doi:10.1175/1520-0442(2000)013<1000:AMITEC>2.0.CO;2.

Uppala, S. M., P. Kållberg, A. Simmons, U. Andrae, V. Bechtold, M. Fiorino, J. Gibson, J. Haseler, A. Hernandez, and G. Kelly (2005), The ERA-40 reanalysis, *Q. J. R. Meteorol. Soc.*, *131*(612), 2961–3012, doi:10.1256/qj.04.176.

Wallace, J. M., and D. S. Gutzler (1981), Téléconnexions in the geopotential height field during the Northern Hemisphere winter, *Mon. Weather Rev.*, *109*(2), 784–812, doi:10.1175/1520-0493(1981)109<0784:TITGHF>2.0.CO;2.

Wang, B. (2006), *The Asian Monsoon*, 781 pp., Praxis, Chichester, U. K.

Wang, B., R. Wu, and X. Fu (2000), Pacific-east Asian teleconnection: How does ENSO affect East Asian climate?, *J. Clim.*, *13*(9), 1517–1536, doi:10.1175/1520-0442(2000)013<1517:PEATHD>2.0.CO;2.

Wang, H., and S. He (2012), Weakening relationship between East Asian winter monsoon and ENSO after mid-1970s, *Chin. Sci. Bull.*, *57*, 3535–3540, doi:10.1007/s11434-012-5285-x.

Wang, M., and J. E. Overland (2009), A sea ice free summer Arctic within 30 years?, *Geophys. Res. Lett.*, *36*, L07502, doi:10.1029/2009GL037820.

Watanabe, M., and T. Nitta (1999), Decadal changes in the atmospheric circulation and associated surface climate variations in the Northern Hemisphere winter, *J. Clim.*, *12*(2), 494–510, doi:10.1175/1520-0442(1999)012<0494:DCITAC>2.0.CO;2.

Wu, B., and J. Wang (2002), Winter Arctic oscillation, Siberian High and East Asian winter monsoon, *Geophys. Res. Lett.*, *29*(19), 1897, doi:10.1029/2002GL015373.

Wu, B., and R. Huang (1999), Effects of the extremes in the North Atlantic Oscillation on East Asia winter monsoon (in Chinese), *Chin. J. Atmos. Sci.*, *26*(6), 641–651.

Yang, L., and B. Wu (2013), Interdecadal variations of the East Asian winter surface air temperature and possible causes, *Chin. Sci. Bull.*, doi:10.1007/s11434-013-5911-2.

Yang, S., K.-M. Lau, and K.-M. Kim (2002), Variations of the East Asian jet stream and Asian-Pacific-American winter climate anomalies, *J. Clim.*, *15*, 306–325, doi:10.1175/1520-0442(2002)015<0306:VOTEAJ>2.0.CO;2.

Yang, S., and W. J. Gutowski (1994), GCM simulations of the three-dimensional propagation of stationary waves, *J. Clim.*, *7*, 414–433.

Zhang, R., A. Sumi, and M. Kimoto (1996), Impact of El Niño on the East Asian monsoon: A diagnostic study of the '86/87 and '91/92 events, *J. Meteorol. Soc. Jpn.*, *74*(1), 49–62.

Zhang, Y., K. R. Sperber, and J. S. Boyle (1997), Climatology and interannual variation of the East Asian winter monsoon: Results from the 1979–95 NCEP/NCAR reanalysis, *Mon. Weather Rev.*, *125*(10), 2605–2619, doi:10.1175/1520-0493(1997)125<2605:CAIVOT>2.0.CO;2.

Zhou, W., X. Wang, T. Zhou, C. Li, and J. C. L. Chan (2007), Interdecadal variability of the relationship between the East Asian winter monsoon and ENSO, *Meteorol. Atmos. Phys.*, *98*(3–4), 283–293, doi:10.1007/s00703-007-0263-6.